

Proceedings of the 16th Czech and Slovak Conference on Magnetism, Košice, Slovakia, June 13–17, 2016

The Effect of Sm Addition on the Microstructure and Superconducting Properties of YBCO Bulk Superconductors

D. VOLOCHOVÁ^{a,*}, P. DIKO^a, S. PIOVARČI^a, V. ANTAL^a, J. KOVÁČ^a AND M. JIRSA^b

^aInstitute of Experimental Physics, SAS, Watsonova 47, 040 01 Košice, Slovakia

^bInstitute of Physics, Czech Academy of Sciences, Na Slovance 2, CZ-18221 Praha 8, Czech Republic

The effect of Sm addition on the microstructure and superconducting properties of Y–Ba–Cu–O (YBCO) bulk superconductors has been studied. Nominal composition: 1 mol $\text{YBa}_2\text{Cu}_3\text{O}_{7-\delta}$ + 0.25 mol Y_2O_3 + 1 wt% CeO_2 was enriched with different amounts of $\text{SmBa}_2\text{Cu}_3\text{O}_y$ powder with the aim to increase critical current density, J_c , especially in higher magnetic fields by introducing additional pinning centers. Single grain YBCO bulk superconductors with $\text{SmBa}_2\text{Cu}_3\text{O}_y$ (Y123-Sm) addition were prepared by the optimized top seeded melt growth process. Microstructure analysis, performed by polarized light microscope, revealed that $\text{SmBa}_2\text{Cu}_3\text{O}_y$ addition leads to a higher amount of slightly coarser Y_2BaCuO_5 particles, which is related to lower critical current densities ($J_c \approx 6 \times 10^4 \text{ A/cm}^2$) of the YBCO samples with $\text{SmBa}_2\text{Cu}_3\text{O}_y$ addition in low magnetic fields. On the other hand, an enhancement of critical current density, J_c , in higher magnetic fields was observed for Y123-Sm samples. Moreover, a maximum trapped magnetic field, B_{tmax} , of 564 mT at 77 K in Y123-Sm, $x = 0.0025$ sample ($\varnothing 17.2 \text{ mm}$) was 43% higher than that for YBCO sample without any addition.

DOI: [10.12693/APhysPolA.131.1009](https://doi.org/10.12693/APhysPolA.131.1009)

PACS/topics: 74.72.-h, 74.62.Dh, 81.10.Fq, 61.72.-y, 74.25.Ha, 74.25.Sv

1. Introduction

Various practical applications of Y–Ba–Cu–O (YBCO) bulk superconductors are mainly based on their ability to trap large magnetic fields [1, 2]. It has already been shown that these materials can trap magnetic field by order of magnitude higher than the best ferromagnets [3]. Recently, Durrell et al. have reported the largest trapped field to date of 17.6 T at 26 K, in a stack of two Gd–Ba–Cu–O (GdBCO) superconducting bulks ($\varnothing 25 \text{ mm}$) [4].

Generally, the magnitude of trapped magnetic field in a bulk superconductor is proportional to the critical current density, J_c , and a diameter of a single grain sample. As a results, general processing aims of these materials consist in an enhancement of critical current density, J_c , of large single grain bulks.

The top seeded melt growth (TSMG) process well accomplishes the second requirement and large single grain YBCO bulk superconductors up to 10 cm in diameter have been fabricated by this process [5]. Additionally, an enhancement of the critical current density, J_c , can be reached by controlling the size, volume fraction, and distribution of secondary phase particles, very often Y_2BaCuO_5 (Y-211) [6] or $\text{Y}_2\text{Ba}_4\text{CuMO}_z$ (Y-2411, $M = \text{Nb, Ta, Mo, W, and others}$) [7]. Besides, it is possible to introduce the additional pinning centers for example by irradiation [8] or by chemical substitutions in a crystal lattice of a superconductor. In later case, different powder additions have been tested, for example Bi_2O_3 [9], NiFe_2O_4 [10], Pr_6O_{11} [11], or Li_2CO_3 [12] leading in most cases to an increase of critical current density, J_c , and trapped magnetic field, B_t .

We report on the microstructure and superconducting properties of YBCO bulk superconductors with Sm addition where substitutions of Ba by Sm are supposed. The influence of Sm addition in the form of $\text{SmBa}_2\text{Cu}_3\text{O}_y$ (Sm-123) on Y-211 particles, critical transition temperature, T_c , critical current density, J_c , as well as trapped magnetic field, B_t , is shown.

2. Experimental details

Two sets of YBCO single grain bulk superconductors without any addition (Y123) and with $\text{SmBa}_2\text{Cu}_3\text{O}_y$ (Y123-Sm) powder addition were prepared by the TSMG process in air. 1 mol $\text{YBa}_2\text{Cu}_3\text{O}_7$, 0.25 mol Y_2O_3 and 1 wt% CeO_2 powders with $Z \text{ wt}\%$ of $\text{SmBa}_2\text{Cu}_3\text{O}_y$ ($Z = 2 \div 10 \text{ wt}\%$ which was supposed to correspond to: $x = 0.001, 0.0025, 0.005, 0.01, 0.02, 0.05$ in $\text{Y}(\text{Ba}_{1-x}\text{Sm}_x)_2\text{Cu}_3\text{O}_{7-\delta}$) were used in nominal composition of the Y123-Sm samples. Precursor powders were mixed for 30 min in a mixer and then intensively milled for 15 min in a friction mill. The mixed powders were uniaxially pressed into the cylindrical pellets of 20 mm in diameter. The samples were treated in a chamber furnace using the following time temperature regime: heating up to $940^\circ\text{C}/\text{dwell } 24 \text{ h}$, heating up to the maximum temperature $1040^\circ\text{C}/\text{dwell } 1 \text{ h}$, fast cooling to a temperature 12°C higher than the temperature of isothermal growth, $T_{is} = 998^\circ\text{C}$ ($T_{is} = 1006^\circ\text{C}$ for the samples Y123-Sm, $x = 0.02$ and 0.05), slow cooling to the isothermal hold temperature, T_{is} , dwell 20 h, slow cooling to 944°C and finally cooling to the room temperature with furnace. For the TSMG process $\text{NdBa}_2\text{Cu}_3\text{O}_z$ single crystals were used as nucleation seeds.

The microstructure of the cross-section of the as-grown samples along the crystallographic c direction was studied by polarized light microscope.

*corresponding author; e-mail: volochova@saske.sk

Small specimens for oxygenation process, performed at 400 °C for 200 h in a flowing oxygen atmosphere, and magnetization measurements were cut 0.5 mm below the top surface of the a -growth sector of prepared bulks at a distance of 3 mm from the seed. They had a shape of a slab with the dimensions $1.5 \times 1.5 \times 0.5 \text{ mm}^3$. The smallest dimension was parallel to the c -axis of the crystal.

The magnetization measurements were performed by a vibrating sample magnetometer with magnetic fields up to 6 T applied parallel to the c -axis of the crystal, at the temperature of 77 K. The critical current densities, J_c , were calculated using the extended Bean model for a rectangular sample [13]. The critical transition temperatures, T_c , were determined from the magnetic transition curves at 50% of the low temperature magnetization. The magnetizations were measured in an applied external magnetic field of 2 mT after zero field cooling. The transition widths, ΔT_c , were determined from the same curve subtracting the 90% and 10% of the low temperature magnetization.

The trapped magnetic field distribution of the bulk samples, oxygenated at 400 °C for 200 h in a flowing oxygen atmosphere, was mapped by the Hall probe sensor. The samples were cooled to liquid nitrogen temperature, in a magnetic field of 1.4 T applied parallel to the c -axis. The trapped field profiles were scanned 15 min after switching the external field off at a distance of 0.1 mm from the sample surface.

3. Results and discussion

Figure 1 shows the top surface macrographs of the Y123 (without any addition) (a) and Y123-Sm, $x = 0.0025$ (Sm-123 addition) (b) single grain samples prepared by the optimized TSMG process. No spontaneous parasitic grain nucleation was observed showing the suitability of the used TSMG process. Additionally, a shrinkage from an initial diameter of the pellet of 20 mm to a diameter of 17.2 mm of the final bulk samples was observed. It should be note that a shrinkage is a typical feature of the samples prepared by the TSMG process and is related to the release of gases present in the pressed pellet as well as oxygen gases which are a product of chemical reactions during the fabrication process. Moreover, a slight loss of a melt, mainly during the dwell at maximum temperature ($T_{\text{max}} = 1040 \text{ °C}$), may contribute to a shrinkage.

In order to determine the influence of Sm addition (in the form of Sm-123 powder) on the superconducting properties, a series of magnetization measurements was performed on prepared samples using a vibrating sample magnetometer. It should be noted that all the specimens were cut from the equivalent position within the bulk (as described in Sect. 2) and they were all oxygenated at same time under the same thermal conditions in order to keep the comparison meaningful.

The results of the magnetization measurements are summarized in Fig. 2 and Fig. 3. The critical temperatures, T_c , of the samples with different Sm concentrations

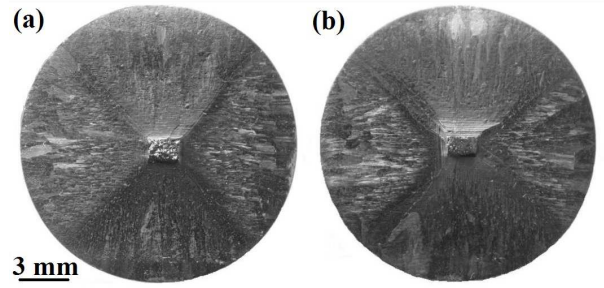


Fig. 1. Top surface macrographs of Y123 (a) and Y123-Sm, $x = 0.0025$ (b) single grain samples prepared by the TSMG process. The diameter of the samples was 17.2 mm.

were not found to be significantly influenced by Sm-123 addition when compared to Y123 sample without any addition ($x = 0$, $T_c = 90.9 \text{ K}$). Moreover, Sm-123 addition in the studied range does not influence the width of superconducting transition, ΔT_c , and ΔT_c is around 0.5 K for all samples.

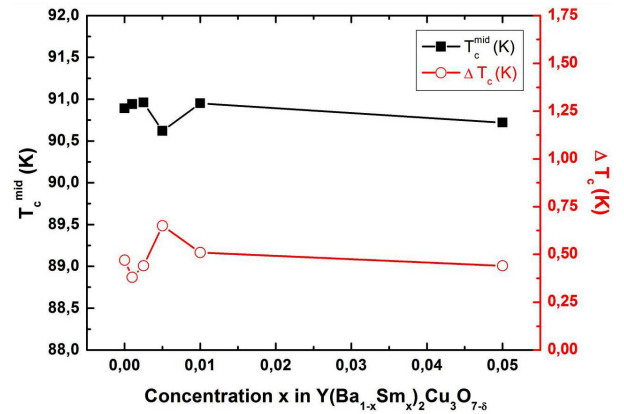


Fig. 2. T_c and ΔT_c values as a function of Sm concentration, x , for the YBCO samples with Sm-123 addition (Y123-Sm).

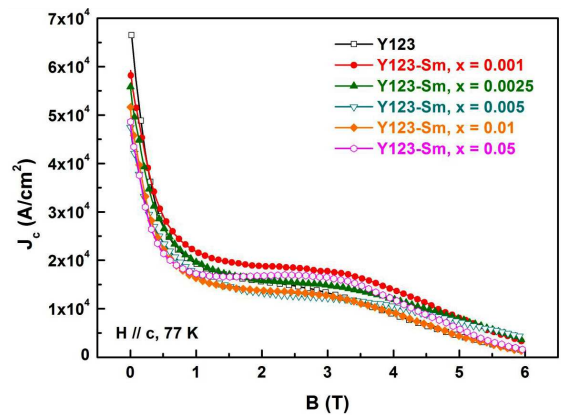


Fig. 3. Field dependences of the critical current density at 77 K and $H \parallel c$ of the samples without addition (Y123) and samples with Sm-123 addition (Y123-Sm).

Microstructure analysis, performed by polarized light microscope, revealed that Sm-123 addition leads to a higher amount of slightly coarser Y-211 particles (Fig. 4), which is related to lower critical current densities ($J_c(0 \text{ T}, 77 \text{ K}) \approx 6 \times 10^4 \text{ A/cm}^2$) of the YBCO samples with Sm-123 addition in low magnetic fields when compared to YBCO sample without any addition ($J_c(0 \text{ T}, 77 \text{ K}) = 6.6 \times 10^4 \text{ A/cm}^2$) [6].

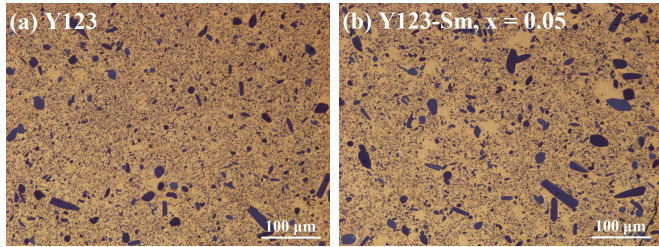


Fig. 4. Microstructure of the Y123 sample without any addition (a) and the Y123-Sm, $x = 0.05$ (b).

On the other hand, an enhancement of critical current density, J_c , in higher magnetic fields was observed for Y123-Sm, $x = 0.001, 0.0025, 0.05$ samples. The enhancement of J_c may suggest the presence of some additional pinning centers created by Sm substitutions.

In spite of relatively low enhancement of J_c , all the samples with Sm-123 addition possess a trapped magnetic field higher than that for YBCO sample without any addition (Table I). A maximum trapped magnetic field, $B_{t \max}$, of 564 mT at 77 K in Y123-Sm, $x = 0.0025$ sample ($\varnothing 17.2 \text{ mm}$) was of 43% higher than that for YBCO sample without any addition (Fig. 5).

TABLE I

Dependence of the maximum trapped field, $B_{t \max}$, of the Y123-Sm single grain samples on the concentration of Sm, x .

| Concentr. x | 0 | 0.001 | 0.0025 | 0.005 | 0.01 | 0.02 |
|-------------------|-----|-------|--------|-------|------|------|
| $B_{t \max}$ [mT] | 395 | 462 | 564 | 513 | 500 | 504 |

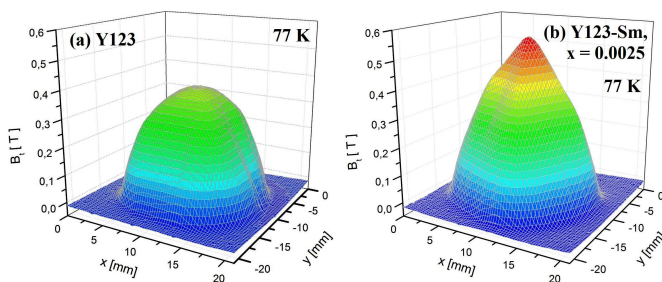


Fig. 5. Profile of trapped magnetic field at 77 K in the Y123 sample without addition, $B_{t \max} = 395 \text{ mT}$ (a) and in the Y123-Sm, $x = 0.0025$, $B_{t \max} = 564 \text{ mT}$ (b). The macrostructure of the as-grown samples is shown in Fig. 1.

4. Conclusions

YBCO bulk superconductors with Sm addition were prepared by the optimised TSMG process in the form

of single grains. The critical temperatures, T_c , as well as the width of superconducting transitions, ΔT_c , were not found to be significantly influenced by Sm addition. Microstructure analyses revealed that Sm-123 addition leads to a higher amount of slightly coarser Y-211 particles, which is related to lower critical current densities of the Y123-Sm samples in low magnetic fields when compared to YBCO sample without any addition. On the other hand, an enhancement of critical current density, J_c , in higher magnetic fields was observed for Y123-Sm, $x = 0.001, 0.0025, 0.05$ samples. Higher values (up to 43%) of the maximum trapped magnetic fields measured in all the Y123-Sm samples represent a positive influence of Sm addition on properties of YBCO bulk superconductors.

Acknowledgments

This work was realized within the framework of the projects: ITMS 26220120019, ITMS 26220120035, ITMS 26220220061, ITMS 26220220041, ITMS 26110230097, ITMS 26110230061, APVV No. 0330-12, VEGA No. 2/0121/16, Stefanik Project SK-FR-2013-0025 and SAS Centre of Excellence: CFNT MVEP.

References

- [1] G. Fuchs, P. Schätzle, G. Krabbes, S. Gruf, P. Verges, K.-H. Müller, J. Fink, L. Schultz, *Appl. Phys. Lett.* **76**, 2107 (2000).
- [2] F.N. Werfel, U. Floegel-Delor, R. Rothfeld, T. Riedel, B. Goebel, D. Wippich, P. Schirrmeister, *Supercond. Sci. Technol.* **25**, 014007 (2012).
- [3] M. Tomita, M. Murakami, *Nature* **421**, 517 (2003).
- [4] J.H. Durrell, A.R. Dennis, J. Jaroszynski, M.D. Ainslie, K.G.B. Palmer, Y.-H. Shi, A.M. Campbell, J. Hull, M. Strasik, E.E. Hellstrom, D.A. Cardwell, *Supercond. Sci. Technol.* **27**, 082001 (2014).
- [5] R. Tournier, E. Beaugnon, O. Belmont, X. Chaud, D. Bourgault, D. Isfort, L. Porcar, P. Tixador, *Supercond. Sci. Technol.* **13**, 886 (2000).
- [6] M. Murakami, K. Yamaguchi, H. Fujimoto, N. Nakamura, T. Taguchi, N. Koshizuka, S. Tanaka, *Cryogenics* **32**, 930 (1992).
- [7] N. Hari Babu, K. Iida, Y. Shi, T.D. Withnell, D.A. Cardwell, *Supercond. Sci. Technol.* **19**, S461 (2006).
- [8] R. Gonzalez-Arrabal, M. Eisterer, H.W. Weber, G. Fuchs, P. Verges, G. Krabbes, *Appl. Phys. Lett.* **81**, 868 (2002).
- [9] W.M. Yang, M. Wang, *Physica C* **493**, 128 (2013).
- [10] G.-Z. Li, L. Dong, X.-Y. Deng, *J. Am. Ceram. Soc.* **99**, 388 (2016).
- [11] X.Q. Xu, Y.Q. Cai, C.X. Yang, X. Yao, S. Xu, A. Kortyka, R. Puzniak, *Supercond. Sci. Technol.* **22**, 015001 (2009).
- [12] L. Shlyk, G. Krabbes, G. Fuchs, K. Nenkov, P. Verges, *Physica C* **392-396**, 540 (2003).
- [13] D.-X. Chen, R.B. Goldfarb, *J. Appl. Phys.* **66**, 2489 (1989).